The shapes and sizes of two-dimensional pressurized self-intersecting rings, as models for two-dimensional vesicles

1993 J. Phys. A: Math. Gen. 26 1

(http://iopscience.iop.org/0305-4470/26/1/006)

J. Phys. A: Math. Gen. 26 (1993) 1-13. Printed in the UK

The shapes and sizes of two-dimensional pressurized, self-intersecting rings, as models for two-dimensional vesicles

George Gaspari†, Joseph Rudnick‡ and Arezki Beldjenna‡

† Physics Department, University of California, Santa Cruz, Santa Cruz, CA 95064, USA
‡ Department of Physics, UCLA, Los Angeles, CA 90024-1547, USA

Received 26 March 1992

Abstract. Two-dimensional vesicles are modelled as pressurized, unrestricted closed random walks. The model, though suffering from undesirable physical characteristics, has the decided advantage of yielding exact analytical statistical analysis of the size and shapes of these objects. Closed-form expressions for the average of the square of the radius of gyration and the asphericity are derived. In addition, exact expressions for the full probability distribution are also obtained. Numerical computations of the probability function for several pressures are presented. We arrive at a new, exact formula for the distribution function, $P(R_1^2, R_2^2)$, of the principal components of the square of the radius of gyration for two-dimensional rings.

1. Introduction

Membranes consisting of closed bilayer sheets of lipid molecules are known as vesicles. Their shapes were first successfully interpreted in the pioneering work of Canham (1970), Helfrich (1973) and Deuling and Helfrich (1976). In these studies, it was recognized that vesicles in equilibrium, such as red blood cells, assume a shape that minimizes distortional energy. It was argued that the dominant distortional force is due to bending. Other forces related to stretching or tilting play a secondary role in influencing the shapes of the membranous surface of these vesicles. The most probable shape of a vesicle is, then, determined by minimizing an appropriate curvature energy. This procedure leads to vesicle surfaces determined by an Euler-Lagrange equation. The situation is slightly more involved if the vesicles find themselves in a fluid at finite temperature where an osmotic pressure differential is maintained. Now the shape of the cell will fluctuate. In thermodynamic equilibrium, the probability distribution of the membrane's shape will be described by the laws of statistical mechanics. A calculation based on this approach was first carried out by Ostrowsky and Peyrand (1982).

More recently, Leibler, Fisher and co-workers (1987, 1989, 1990 and 1991) have engaged in a comprehensive numerical investigation of the two-dimensional vesicle, which is modelled as a closed, self-avoiding two-dimensional random walk acted on both by bending forces and by a force due to an effective osmotic pressure difference $\Delta p = p_{\text{int}} - p_{\text{ext}}$ between the fluid inside the closed walk and that of the external environment. The two regimes, an 'inflated' regime corresponding to $\Delta p > 0$, and a 'deflated' regime, which corresponds to $\Delta p < 0$, were both studied by these authors.

0305-4470/93/010001+13$07.50

In addition to Monte Carlo calculations of wall conformation as a function of pressure, Leibler *et al* were able to identify important scaling properties of various shape parameters.

It was noticed by Rudnick and Gaspari (1991) that the relaxation of the requirement of self-avoidance in the random walk model of Leibler *et al* transforms the system from one that can only be attacked numerically to one whose statistical mechanics are amenable to a complete analytical solution. This 'phantom wall' model allows for configurations in which the wall of a vesicle intersects itself; although such configurations are clearly ruled out on physical grounds the incorporation of this theoretical defect has the advantage of yielding a tractable model of two-dimensional vesicles subject to a pressure differential. In particular, the distribution of the shapes of these vesicles can be *exactly* determined. Models like this one (physically unrealistic in one or more ways, but exact solvable) have historically played an important role in guiding theoretical and conceptual progress. It is in this spirit that we introduce the present model.

In section 2, the model is described, and the statistical analysis is presented. This section will be devoted to the formulation of the theory and to deriving specific results that have, in large part, already appeared in the literature (Rudnick and Gaspari 1991). New findings are presented in section 3. We arrive at a closed, exact expression for $P(\lambda_1, \lambda_2)$, the probability density for the two principal components of the radius of gyration (Solĉ 1971) of a polymer ring under pressure. A detailed numerical study of the probability density as a function of pressure will be presented. Concluding remarks appear at the end of section 3. An appendix discusses the influence of self-avoidance on the configurational statistics of the two-dimensional vesicle when the internal pressure excess is almost sufficient to cause it to expand without limit, or 'pop'. We find that there is a regime in which self-avoidance plays at most a perturbative role.

In a subsequent paper we will discuss the non-equilibrium properties of this model for two-dimensional vesicles.

2. Two-dimensional pressurized vesicles

2.1. The model

The vesicle is pictured as an N-sided irregular polygon. The edges of this figure are permitted to cross, and the statistics governing the distribution of the angle between adjacent sides are assumed to be those of an unrestricted random walk in two dimensions. When there is no pressure differential these random walks can, in the limit of large N, be modelled as random flights obeying Gaussian statistics. If Δ^2 is the mean square length of a link, η, then the probability distribution governing η, here a two-dimension vector, is

$$P(\eta_{\alpha i}) = \left(\frac{1}{\Delta^2 \pi}\right)^{1/2} \exp(-\eta_{\alpha i}^2/\Delta^2) \tag{1}$$

and

$$\sum_{i=1}^{2} \langle \eta_{\alpha i}^2 \rangle = \Delta^2 \qquad \alpha = 1, 2, \ldots . \tag{2}$$

The probability distribution of any shape specified by a set of displacements η_α is

then given by the product

$$\prod_{\alpha=1}^{N}\prod_{i=1}^{2} P(\eta_{\alpha i}).$$

An additional Botzmann factor, $\exp(\Delta pA/kT)$, is required when the osmotic pressure differential is not zero. The quantity A is the area enclosed by the bounding wall. In calculating the averages, the constraining equations relating the η_αs must be taken into account. In the present situation, the requirement that the walk is closed demands that the displacements sum to zero. This leads to two constraint equations:

$$\sum_{\alpha=1}^{N} \eta_{\alpha i} = 0 \qquad i = 1, 2. \tag{3}$$

At this point one has a choice: the calculation can either be carried out in a constant pressure or a constant area ensemble. Since the constant pressure ensemble is the more relevant one experimentally, we carry through the analysis in that ensemble. Pertinent results for the constant area ensemble will be presented when they are useful.

Bending forces can be accommodated through the inclusion of the factor $\exp(-E_b/kT)$ where the bending energy takes on the form

$$E_b = \frac{\kappa}{2\Delta^2}\sum_i (\eta_{i+1} - \eta_i)^2$$

κ being the rigidity constant. It is a straightforward matter to show, at least in the inflated regime, that when the rigidity persistence length, $\Delta kT/\kappa$, is smaller than either the length of the bounding wall, $N\Delta$, or the pressure persistence length, $kT/\Delta(\Delta p)$, the statistical properties are unaffected by bending forces, except for a renormalization of the effective length of a link. These observations are borne out by the numerical results of Leibler *et al.*

We now argue that the $\Delta p > 0$ region is the only one pertinent to our model, thereby justifying the neglect of the bending term, at least for small rigidity. Using Green's theorem, the probability is expressible in terms of the displacements. Specifically, for flat surfaces the area, A, is equal to the line integral $\frac{1}{2}\oint (y\,\mathrm{d}x - x\,\mathrm{d}y)$ along the bounding curve. Note that the integral has a sign associated with the direction of integration, so closed paths that are flipped give contributions of opposite sign, which is equivalent to changing the sign of the pressure. In this model, then, the deflated regime is inaccessible; $\Delta p > 0$ and $\Delta p < 0$ both correspond to pressures that tend to inflate the vesicle.

Evaluating the line integral along the polygon, one obtains the following expression for the area

$$A = \tfrac{1}{2}\sum_{\alpha\alpha'=1}^{N} \eta_{\alpha x}\eta_{\alpha' y}\phi(\alpha - \alpha'). \tag{4}$$

The function $\phi(x)$ is the step function, $\phi(x) = x/|x|$. It is convenient to introduce a dimensionless quantity $p \equiv \Delta^2(\Delta p/kT)$ and to consider the coordinates to be a set expressed in units of Δ^2. Then, using (4), the probability density is written

$$P(\eta_1, \eta_2, \ldots) = \frac{1}{Z}\exp\left(-\sum_\alpha (\eta_{\alpha x}^2 + \eta_{\alpha y}^2) + \frac{p}{2}\sum_{\alpha\alpha'} \eta_{\alpha x}\eta_{\alpha y}\phi(\alpha - \alpha')\right). \tag{5}$$

The quantity Z normalizes the probability. The essential observation is that the exponent has a bilinear form in the η's. Because of this, Gaussian statistics hold. The

expression in the exponent is easily diagonalized on Fourier transforming the coordinates. A suitable set is defined by

$$\eta_{\alpha x} = \sum_k \sqrt{\frac{2}{N}} (A_k \cos(\alpha k) + B_k \sin(\alpha k)) \tag{6a}$$

$$\eta_{\alpha y} = \sum_k \sqrt{\frac{2}{N}} (A'_k \cos(\alpha k) + B'_k \sin(\alpha k)) \tag{6b}$$

where $k = 2\pi n/N$ $(n = 1, 2, \ldots, N)$. Note that because of the constraint of net zero displacement the $k = 0$ term is not present in the sum. In terms of these variables, the probability function becomes

$$P(\ldots A_k, B_k, A'_k, B'_{k'} \ldots) = \frac{1}{Z} \exp\left(\sum_k -(A_k^2 + B_k^2 + A_k'^2 + B_k'^2) + p \sum_k \frac{B_k A'_k - A_k B'_k}{k} \right). \tag{7}$$

The final step in the diagonalizing process is tantamount to finding the eigenvalues of the 4×4 matrix that couples the Fourier amplitudes. Once this has been accomplished ensemble averaging reduces to the evaluation of simple Gaussian integrals.

2.2. *The probability density of the principal components of the radius of gyration*

The gyration tensor, $\boldsymbol{T}$, turns out to be a central quantity in the description of the size and shape of irregular bodies (Solĉ and Stockmayer 1971. See also Gaspari *et al* 1987). In terms of the displacement vectors, its components have the compact form (Forsman and Hughes 1963)

$$T_{ij} = \Delta^2 \sum_{\alpha\beta} a_{\alpha\beta} \eta_{\alpha i} \eta_{\beta j} \tag{8}$$

with the elements of the symmetric matrix $a_{\alpha\beta}$ given by

$$\begin{aligned} a_{\alpha\beta} &= \frac{1}{(N+1)^2} \alpha(N+1-\beta) \qquad \alpha > \beta \\ \alpha_{\alpha\beta} &= \frac{1}{(N+1)^2} \beta(N+1-\alpha) \qquad \beta > \alpha. \end{aligned} \tag{9}$$

In two dimensions, $\boldsymbol{T}$ is a 2×2 matrix with two eigenvalues, λ_1 and λ_2. Two useful invariants that provide a rough measure of the extent of an object and its deviation from spherical symmetry are the square of the radius of gyration and the asphericity (Rudnick and Gaspari 1986), defined by

$$\begin{aligned} R^2 &= \lambda_1 + \lambda_2 \\ A_2 &= \frac{(\lambda_1 - \lambda_2)^2}{(\lambda_1 + \lambda_2)^2}. \end{aligned} \tag{10}$$

These quantities must be averaged for random objects, such as vesicles. Complete statistical information is, of course, contained in the probability density of the principal components λ_1 and λ_2 from which averages can be calculated, including $\langle R^2 \rangle$ and $\langle A_2 \rangle$. We turn to that probability function.

In an earlier report (Rudnick and Gaspari 1991), an exact expression for $P(\lambda_1, \lambda_2)$ was presented:

$$P(\lambda_1, \lambda_2)/2 = |\lambda_1 - \lambda_2| \int \delta(\lambda_1 + \lambda_2 - T_{xx} - T_{yy}) \delta((\lambda_1 - \lambda_2)^2 - (T_{xx} - T_{yy})^2 - 4T_{xy}^2) \times P(A_1, B_1 \ldots A'_1 B'_1 \ldots)\, \mathrm{d}A_1 \ldots \tag{11}$$

where the integral is over all Fourier variables. Replacing the delta functions by their representation as Fourier integrals, yields an expression in terms of integrals and sums over simple functions. Unfortunately, no such treatment for the probability density is known for dimension other than two. Explicit evaluation of (11) is deferred to section 3.

To evaluate the average of the square of the radius of gyration, $\langle R^2 \rangle$, a simpler, but somewhat less informative statistical distribution, $P(R^2)$ is all that is needed. It is defined by

$$P(R^2) = \int \delta(R^2 - T_{xx} - T_{yy}) P(A_1, B_1 \ldots A_1' B_1' \ldots)\, \mathrm{d}A_1\, \mathrm{d}B_1 \ldots \mathrm{d}A_1'\, \mathrm{d}B_1' \ldots . \tag{12}$$

In order to carry out the integration in (12) we express the components of the gyration tensor in terms of the Fourier amplitudes; noting that for large N

$$\begin{aligned} \sum_\beta a_{\alpha\beta} \cos k\beta &= \frac{1}{N} \frac{\cos k\alpha}{k^2} - \frac{1}{Nk^2} \\ \sum_\beta a_{\alpha\beta} \sin k\beta &= \frac{1}{N} \frac{\sin k\alpha}{k^2}. \end{aligned} \tag{13}$$

Then, using equations (6), (8) and (13) we obtain the following relationships

$$\begin{aligned} T_{xx} &= \sum_k \frac{\Delta^2}{Nk^2} (A_k^2 + B_k^2) \\ T_{yy} &= \sum_k \frac{\Delta^2}{Nk^2} (A_k'^2 + B_k'^2) \end{aligned} \tag{14}$$

and

$$T_{xy} = T_{yx} = T_{xx} = \sum_k \frac{\Delta^2}{Nk^2} (A_k A_k' + B_k B_k').$$

The integral becomes, on writing the delta function as a Fourier integral,

$$\begin{aligned} P(R^2) = \frac{1}{2\pi Z} \int \mathrm{d}\omega \exp(\mathrm{i}\omega R^2) \int \exp\Bigg(\sum_k - \Bigg(1 + \frac{\mathrm{i}\omega\Delta^2}{k^2} \Bigg) \\ \times (A_k^2 + B_k^2 + A_k'^2 + B_k'^2) - \frac{p}{k} (A_k B_k' - A_k' B_k) \Bigg) \mathrm{d}A_k \ldots . \end{aligned} \tag{15}$$

Completing the Gaussian integrals over the Fourier amplitudes, we are left with

$$\begin{aligned} P(R^2) &= \frac{1}{2\pi Z} \int \exp(\mathrm{i}\omega R^2) \prod_k \frac{1}{1 + \dfrac{\mathrm{i}\omega\Delta^2}{k^2} - \dfrac{p^2}{4k^2}} \\ &= \frac{\pi p_c}{2\pi\Delta^2} \frac{\sin \pi x}{x} \int \exp\Bigg(\mathrm{i} \frac{\pi p_c}{\Delta^2} R^2 \omega \Bigg) \frac{\mathrm{i}\omega\, \mathrm{d}\omega}{\sin \pi \Big(-\dfrac{x}{2} + r \Big) \sin \pi \Big(-\dfrac{x}{2} - r \Big)} \end{aligned} \tag{16}$$

where $r = [(x^2/4) - (\mathrm{i}\omega\Delta^2/\pi p_c)]^{1/2}$, p_c, the critical pressure, is $4\pi/N$ and $x = p/p_c$. The normalization factor Z is given by

$$\begin{aligned} Z^{-1} &= \prod_k \Bigg(1 - \frac{p^2}{4k^2} \Bigg) \\ &= \frac{\sin \pi x}{\pi x}. \end{aligned} \tag{17}$$

This last quantity is just the inverse of the number of closed, pressurized walks of the sort considered here. The final equalities in (16) and (17) are obtained using the standard techniques of contour integration.

Note that in the limit of zero pressure $x \to 0$,

$$P(R^2, x=0) = \frac{\pi^2 p_c}{2\Delta^2} \int \exp\left(i \frac{\pi p_c}{\Delta^2} R^2 \omega \right) \frac{i\omega \, d\omega}{\sin^2 \pi\sqrt{-i\omega}}. \tag{18}$$

This is the two-dimensional version of the result found by Fixman in his study of three-dimensional polymer chains. In contrast to the three-dimensional case, the integral in (18) can be performed explicitly by contour integration. The poles are on the positive imaginary axis, and the contour can be closed in the upper half-plane. On evaluating the residues one obtains

$$P(R^2, x=0) = \frac{2\pi p_c}{2\Delta^2} \sum_{n=1}^{\infty} (3n^2 - 8\pi^2 (R/\Delta)^2 n^4) \exp(-\pi p_c (R/\Delta)^2 n^2). \tag{19}$$

As a check, one can verify that $\int_0^\infty R^2 P(R^2 \, dR^2) = \langle R^2 \rangle = N/12$. In the small and large R^2 regimes (18) can be evaluated by steepest descents, yielding the following asymptotic forms: $P(R^2, x=0) \to \exp(-3\langle R^2 \rangle / R^2)$ $(\langle R^2 \rangle \gg R^2)$ and $P(R^2, x=0) \to \exp[-(\pi^2 R^2/3)/\langle R^2 \rangle]$ $(\langle R^2 \rangle \ll R^2)$. These findings are fully consistent with the exact formula displayed in (19).

When the pressure is non-zero the distribution as given by (16) continues to be amenable to contour integration methods. A straightforward, but more involved analysis leads to the following formula for $P(R^2)$:

$$P(R^2) = \frac{\pi p_c}{\Delta^2} \frac{1}{x} \sum_{n=-\infty}^{\infty} \left\{ (2n - x)(n^2 - nx) \exp\left(-\frac{\pi p_c}{\Delta^2} R^2 n(n-x) \right) \right\}. \tag{20}$$

A discussion of the scaling behaviour of $P(R^2)$ and a numerical evaluation of the sum has been reported previously (Rudnick and Gaspari 1991). The asymptotic behaviour is not substantially modified by pressure, except in the $p \to p_c$ limit, where the vesicle takes on a circular shape. The mean square radius of gyration is now calculated to be

$$\begin{aligned} \langle R^2 \rangle &= \frac{\Delta^2}{\pi p_c} \sum_{n=1}^{\infty} \frac{1}{n^2 - x^2} \\ &= \frac{\Delta^2}{\pi p_c} \left\{ \frac{1}{x^2} - \frac{\pi}{x} \frac{1}{\tan \pi x} \right\} \end{aligned} \tag{21}$$

recovering the result reported earlier (Rudnick and Gaspari 1991). As pointed out in that reference, a closed form expression for $\langle R^2 \rangle$ can also be obtained in the constant area ensemble. The expression takes the scaling form $N\Delta^2 f[A/(N\Delta^2)]$, and it asymptotically approaches the limit A/π as $A \to \infty$. It is instructive to note that all results in the constant pressure ensemble lead almost immediately to corresponding results in the constant area ensemble. One simply replaces the real value, p, by an imaginary one, ip, and utilizes the identity

$$\delta(A - A_0) = \frac{1}{2\pi} \int_{-\infty}^{\infty} e^{ip(A - A_0)} \, dp.$$

Applying this chain of reasoning to the distribution function $P(R^2)$, as defined above,

we obtain

$$P_A(R^2; A_0) = \frac{1}{2\pi} \int_{-\infty}^{\infty} P_p(R^2; -ip)\, e^{-ipA_0}\, dp \tag{22}$$

where the subscripts p and A identify the ensembles as constant pressure and constant area.

2.3. *The asphericity*

As mentioned earlier, an excellent single-parameter measure of the deviation form spherical symmetry of an irregular object, random or otherwise, is the asphericity parameter (Rudnick and Gaspari 1986; see also Theodoru and Suter 1985 and Aronovitz and Nelson 1986) defined for an object embedded in d spatial dimensions as follows:

$$A_d = \frac{1}{d-1} \sum_{j>i}^{d} \frac{\langle (R_i^2 - R_j^2)^2 \rangle}{\langle (\Sigma_{k=1}^{d} R_k^2)^2 \rangle}. \tag{23}$$

In (23) the numerator and denominator are averaged separately. This eases the calculational difficulties, although it is also possible to define, and obtain explicit results for, a version of the asphericity parameter in which the averaging is performed *after* the ratio has been taken. Indeed, Levinson has recently performed such a calculation for vesicles (1992).

In two dimensions the calculation of the asphericity parameter, here A_2, proceeds most simply if one uses the expression (Gaspari *et al* 1987)

$$A_2 = \frac{[\langle T_{xx}^2 \rangle - \langle T_{xx} T_{yy} \rangle] + 2\langle T_{xy}^2 \rangle}{\langle T_{xx}^2 \rangle - \langle T_{xx} T_{yy} \rangle + 2\langle T_{xx} T_{yy} \rangle}. \tag{24}$$

Once again, replacing the elements of the matrix T by their Fourier decompositions, one finds that the averages are straightforward to evaluate: for example

$$\langle T_{xx} T_{xx} \rangle = \frac{\Delta^2}{4N^2} \left\{ \sum_{kk'} \frac{1}{k^2 k'^2} \left(\frac{1}{\lambda_+} + \frac{1}{\lambda_-} \right) \left(\frac{1}{\lambda'_+} + \frac{1}{\lambda'_-} \right) + \sum_k \frac{1}{k^4} \left(\frac{1}{\lambda_+} + \frac{1}{\lambda_-} \right)^2 \right\}. \tag{25}$$

The quantities λ_+ and λ_- are the eigenvalues ($\lambda_\pm = (1 \pm (p/2k))$) of the 4×4 matrix

$$\begin{bmatrix} 1 & 0 & 0 & \frac{p}{2k} \\ 0 & 1 & -\frac{p}{2k} & 0 \\ 0 & -\frac{p}{2k} & 1 & 0 \\ \frac{p}{2k} & 0 & 0 & 1 \end{bmatrix}. \tag{26}$$

The asphericity is then given by

$$A_2 = \frac{\sum_k \frac{1}{k^2} \left(\frac{1}{k^2 - p^2/4} \right)}{\left(\sum_k \frac{1}{k^2 - p^2/4} \right)^2 + \sum_k \frac{1 + p^2/4k^2}{(k^2 - p^2/4)^2}}. \tag{27}$$

Performing the sums in (27) one finds that

$$A_2 = \frac{\dfrac{8}{p^4} - \dfrac{N^2}{6p^2} - \dfrac{2N}{p^3 \tan(Np/4)}}{-\dfrac{8}{p^4} - \dfrac{N^2}{6p^2} + \dfrac{N^2}{2p^2 \sin^2(Np/4)}}. \tag{28}$$

It can be readily verified from (28) that in the limit $p \to p_c = 4\pi/N$ the asphericity of the vesicles approaches zero. Furthermore in the limit of perfect flaccidity, $p = 0$, the asphericity is equal to $\frac{1}{3}$, the result for a two-dimensional, ring-shaped, non-self-avoiding random walk.

As useful as averaged quantities, such as $\langle R^2 \rangle$ and $\langle A_2 \rangle$ are in parametrizing the size and shape of an irregular object, they provide no direct information concerning the distribution of shapes, which is, in general, much more difficult to get a handle on. However, the pressurized random walk model leads to exact formulae for the probability distribution.

3. Full distribution of the principal radii of gyration

The formula for $P(\lambda_1, \lambda_2)$ displayed as equation (11) serves as the starting point for a closed-form expression for the joint probability distribution. As a first step we write

$$\begin{aligned}\delta(\lambda_1+\lambda_2-T_{xx}-T_{yy})\delta((\lambda_1-\lambda_2)^2-(T_{xx}-T_{yy})^2-4T_{xy}^2) \\ \propto \int \exp(\mathrm{i}\omega_1(\lambda_1+\lambda_2-T_{xx}-T_{yy}))\exp(\mathrm{i}\omega_2(\lambda_1-\lambda_2)^2) \\ \times \exp\left(-\frac{R_1^2}{4}-\frac{R_2^2}{4}+\sqrt{-\mathrm{i}\omega_2}\,R_1(T_{xx}+T_{yy})\right) \\ \times \exp(2\sqrt{-\mathrm{i}\omega_2}\,R_2 T_{xy})\,\mathrm{d}\omega_1\,\mathrm{d}\omega_2\,\mathrm{d}R_1\,\mathrm{d}R_2.\end{aligned} \tag{29}$$

Utilizing (8) to express the elements in T in terms of the η_is, expanding the η_is as a Fourier series, as in (6*a*) and (6*b*) and utilizing (7) for the probability distribution of the Fourier components, one is left with a set of Gaussian integrals to perform over the coefficients. These integrations yield the following expression:

$$\begin{aligned}P(\lambda_1,\lambda_2) = \int \cdots \int \mathrm{d}\omega\,\mathrm{d}\Omega\,\mathrm{d}R_1\,\mathrm{d}R_2 \prod_k \frac{1}{\left(1+\dfrac{\mathrm{i}\omega}{Nk^2}\right)+\left(\dfrac{p^2}{4k^2}-\mathrm{i}\Omega\,\dfrac{R_1^2+R_2^2}{N^2k^2}\right)} \\ \times \mathrm{e}^{\mathrm{i}\omega(\lambda_1-\lambda_2)} J_0(\Omega|\lambda_1-\lambda_2|)|\lambda_1-\lambda_2|\end{aligned} \tag{30}$$

where $k = 2\pi n/N$, n is an integer and the product is over $n > 0$. The product can be evaluated with the aid of contour integration techniques. Once the product has been evaluated, a few other straightforward transformations lead to the following expression for the distribution

$$P(\lambda_1,\lambda_2) = \frac{N}{8\pi}\int_0^\infty \mathrm{d}\Omega \int_{-\infty}^{\infty} \mathrm{d}\omega\, \Psi(a_+)\Psi(a_-)\,\mathrm{e}^{\mathrm{i}\omega(\lambda_1-\lambda_2)} J_0(\Omega|\lambda_1-\lambda_2|)|\lambda_1-\lambda_2| \tag{31}$$

where

$$a_\pm = \frac{\mathrm{i}\omega N}{4\pi^2} - \frac{p^2N^2}{32\pi^2} \pm \left[\left(\frac{\mathrm{i}\omega N}{4\pi^2} - \frac{p^2N^2}{32\pi^2}\right)^2 + \frac{\omega^2N^2}{16\pi^4} - \frac{\Omega^2N^2}{16\pi^4}\right]^{1/2}.$$

If we set $p=0$ this expression simplifies to

$$P(\lambda_1,\lambda_2)=\frac{N}{8\pi}\int_0^\infty d\Omega\int_0^\infty d\omega\,\Psi(\omega+\Omega)\Psi(\omega-\Omega)\times e^{i\omega(\lambda_1-\lambda_2)}J_0(\Omega|\lambda_1-\lambda_2|)|\lambda_1-\lambda_2|. \tag{32}$$

In equations (31) and (33) $J_0(x)$ is the zeroth order Bessel function, and

$$\Psi(x)=\frac{(ix)^{1/2}}{\sinh\left(\pi\frac{N}{4\pi^2}(ix)^{1/2}\right)} \tag{33}$$

$P(\lambda_1,\lambda_2)$ as given by (32) represents an exact formula for the full distribution function of the principal components of the radius of gyration of two-dimensional rings. Solč and Gobush (1974) have previously been able to express $P(\lambda_1,\lambda_2)$ exactly for two-dimensional polymer rings. Their expression requires summing over the zeros of zeroth order Bessel functions. Of course, the two expressions must yield identical values for $P(\lambda_1,\lambda_2)$. However, our equation (33) appears to be in a form more amenable to numerical calculation. No exact expression is known for the probability function in dimensions higher than two.

While there seems to be no analytical way to further reduce the double integral in (33), it is possible to extract the leading behaviour of the probability distribution in the limit of large and small values of λ_1 and λ_2. First, we note that the integrand has no singularities as a function of complex ω in the lower half-plane. Singularities in the top half-plane are in the form of simple poles at $\omega=\pm\Omega+4\pi^2n^2/N$ where n is an integer. If $(\lambda_1+\lambda_2)/N\gg1$ then the integral over ω is closed in the top half-plane and the integral is dominated by contributions from the $n=1$ poles. The probability decays as $\exp(-4\pi^2(\lambda_1+\lambda_2)/N)$. If $(\lambda_1+\lambda_2)/N\ll1$ then the ω integration contour can be shifted downwards into the lower half-plane. It is straightforward to solve for the optimal shift. One finds a decay for small $\lambda_1+\lambda_2$ dominated by the exponential factor $\exp(-N/4(\lambda_1+\lambda_2))$. These asymptotic forms are identical to what was previously found for $P(\lambda_1+\lambda_2=R^2)$. A numerical integration of (32) has been performed. The results are displayed, in the form of a three-dimensional plot, in figure 1. The plot clearly indicates that the walks are not spherical on the average. A circular vesicle represents a highly unlikely, in fact exceptional, case in the present model. We believe that this is so when self-avoidance plays a role, but numerical investigations would be required to establish it.

In addition to the calculations described above, we have generated numerical distributions of non-self-avoiding vesicle walls in a variety of pressure regimes. Such distributions are, in fact relatively elementary to generate because of the simple statistics that govern these objects. While the requirement that a random walk closes places a global restriction on it in real space, this restriction is easily implemented in reciprocal space, as described below equations (6*a*) and (6*b*). One generates a set of A_ks, B_ks, A_k's, and B_k's according to the Gaussian distribution in (7), forms $\boldsymbol{T}$ and diagonalizes the matrix. We have constructed distributions of the eigenvalues λ_1 and λ_2 for pressures equal to 0, $0.5p_c$ and $0.999p_c$. The distributions are shown in figures 2(*a*, *b*, *c*). It is noteworthy that the distribution is only weakly affected by the pressure when $p=0.5p_c$. On the other hand, as the pressure approaches the value at which the vesicle becomes unstable, the effect on the distribution is dramatic, as one might well expect. First, the distribution is quite spread-out; its second moment is comparable to its first, so a wide

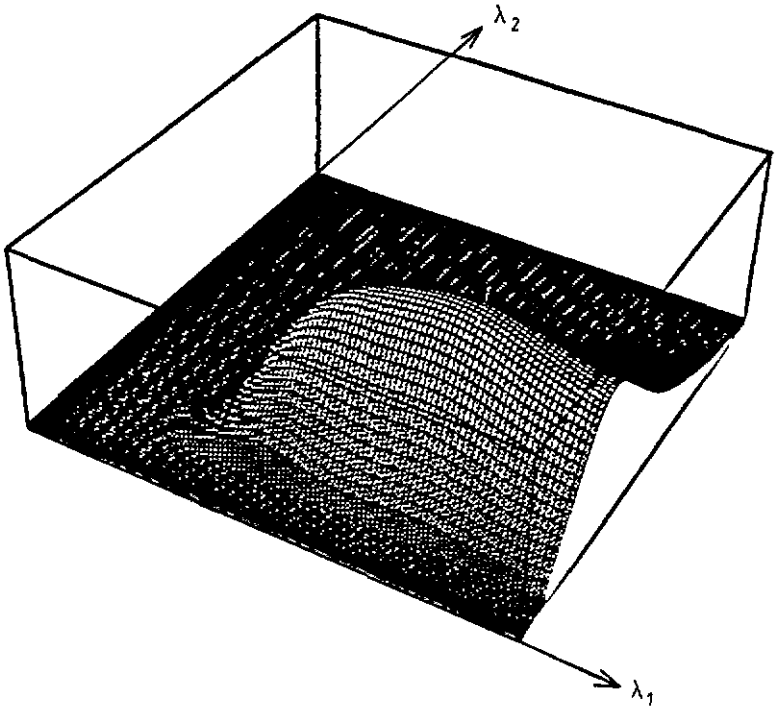

Figure 1. Three-dimensional plot of the joint eigenvalue distribution, $P(\lambda_1, \lambda_2)$, of the moment of inertia tensor of a vesicle with phantom walls, calculated with the use of equations (32) and (33). The vesicle is in a zero pressure environment. The normalization of the eigenvalues is not indicated. The plot was obtained with the use of Mathematica©.

range of values for the eigenvalues is to be expected. This is consistent with results reported earlier for the distribution of the mean radius of gyration (Rudnick and Gaspari 1991). As a second feature, the distribution is peaked in the vicinity of the line $\lambda_1 = \lambda_2$. The highly inflated vesicles are nearly spherical in shape, again in line with reasonable expectations.

4. Conclusions

The model discussed in this paper is a self-contained, analytically tractable representation of two-dimensional vesicles in an environment that includes an osmotic pressure differential. While this representation is several steps removed from realistic models of physical and biological vesicles its solvability enables one to test hypotheses, and to develop additional insight into the behaviour of vesicles in interesting contexts. Furthermore, there may well exist physical realizations of the kind of self-intersecting ring-like system considered here. A polymer ring on a flat surface can, in principle, flip over itself and thus adopt a figure-eight, or similar 'self-intersecting' configuration. In addition, it is shown in the appendix that there is a regime sufficiently close to the critical pressure in which the requirement of self-avoidance is irrelevant to the configurational statistics of the vesicle wall.

The primary purpose of this paper is to elucidate the analytical features of the model, and to illustrate how useful results are extracted. As we hope has been made

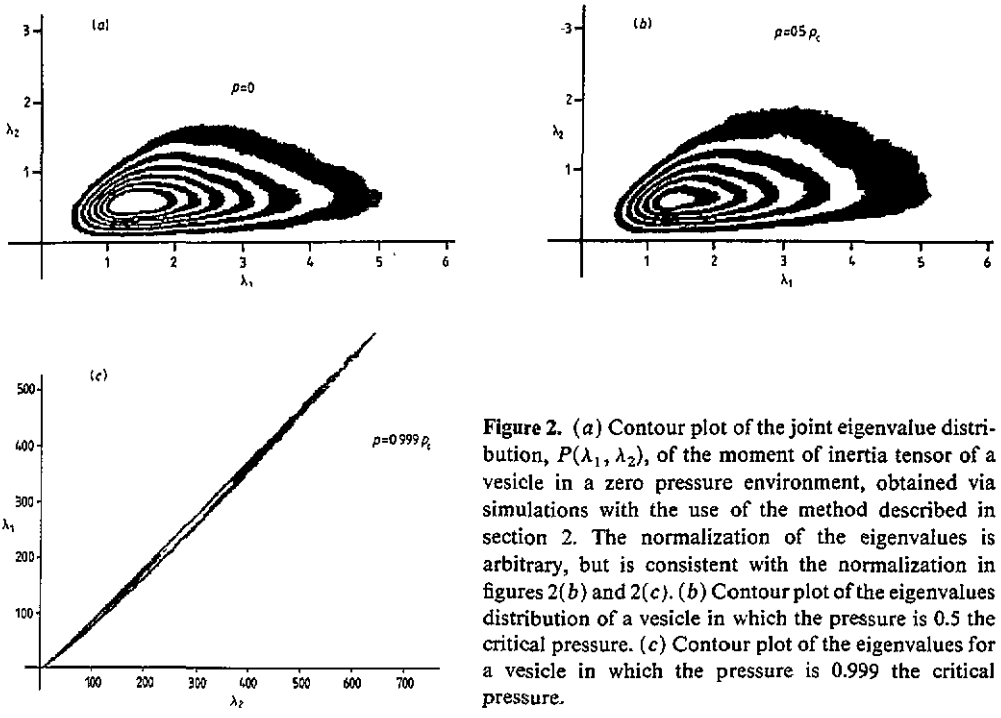

Figure 2. (*a*) Contour plot of the joint eigenvalue distribution, $P(\lambda_1, \lambda_2)$, of the moment of inertia tensor of a vesicle in a zero pressure environment, obtained via simulations with the use of the method described in section 2. The normalization of the eigenvalues is arbitrary, but is consistent with the normalization in figures 2(*b*) and 2(*c*). (*b*) Contour plot of the eigenvalues distribution of a vesicle in which the pressure is 0.5 the critical pressure. (*c*) Contour plot of the eigenvalues for a vesicle in which the pressure is 0.999 the critical pressure.

clear, this process is by no means complicated. The value of this model is thus clear. We believe that it represents an excellent 'zeroth order' theory, which will, we expect, be amenable to some kind of renormalization when the constraint of self-avoidance is introduced. We note here that the influence of bond rigidity can, in principle, be added to this model. Preliminary investigations indicate that the two limiting regimes, the nearly-flaccid regime, in which the rigidity modulus is very small, and the almost-spherical regime, in which the rigidity persistence length is greater than the circumference of the vesicle wall, can be straightforwardly treated. An issue not discussed in this paper, but addressed in an earlier publication (Rudnick and Gaspari 1991), is that of scaling. It is easy to verify that this model exhibits the kind of scaling studied by Maggs *et al* (1991). The exponents are mean-field-like, as one might well expect. Finally, we note here that the model continues to be tractable when suitable dynamics are included. An analytical and numerical investigation of the dynamics of this system is the subject of the following paper (Gaspari *et al* 1993). This remarkable property of the 'phantom wall' vesicle will, one hopes, lead to even further insights into the physical properties of this fascinating system.

Acknowledgments

We are extremely grateful to Mr Mark Fauver, who is responsible for the bulk of the simulations discussed here.

Appendix. Effect of self-avoidance on the statistics of the highly inflated vesicle

Heuristically, one expects that the highly inflated walk will not especially feel the effects of self-avoidance. In a regime in which the vesicle wall is stretched to the

breaking point the energetic cost of the wall's bending back on itself is so great that self-intersection will not play a significant role in conformational statistics. In this appendix, we provide a mathematical basis for that intuition. A calculation in the context of perturbation theory indicates that self-avoidance has a quantitative, not a qualitative effect on vesicle wall statistics near the 'popping' transition, and that, if the pressure is sufficiently close to the critical pressure, there is no need to renormalize the theory beyond simple multiplicative redefinitions. The results derived here also give an indication of how closely one must adjust the pressure to its critical value in order to avoid the necessity of taking self-avoidance into account.

We start by considering the lowest order renormalization of the fugacity, z, in the grand-canonical ensemble. This renormalization is effected by adding to z the expression represented by the diagram displayed in figure A1. The diagram is just the graphical representation of the generating function for the closed, unrestricted walk. With the use of equation (17) we obtain the following result for the renormalized fugacity, z_R:

$$z_R = z + u \sum_{N=1}^{\infty} \frac{\pi p}{\sin(N\pi p)} \left(\frac{z}{z_c}\right)^N \equiv z + uf(z) \tag{A.1}$$

where u is a coupling constant, which is taken to be small. Now we assume that $p_c = 1/N_0$, so the vesicle with N_0 wall sections will pop when subjected to an internal pressure excess greater than p_c. Let $p = p_c(1-\delta)$, where

$$\delta \ll 1/(N_0 \ln(N_0)). \tag{A.2}$$

Then, when $N = N_0$

$$\frac{\pi p}{\sin(N_0 \pi p)} \approx \frac{1}{N_0 \delta} \tag{A.3}$$

and, when $N = N_0 - m$, with $m \geq 1$,

$$\frac{\pi p}{\sin((N_0 - m)\pi p)} \approx \frac{1}{m}. \tag{A.4}$$

Note that the right-hand side of (A.3) will be much greater than the right-hand side of (A.4). Now, in order to obtain the number of closed walks with N_0 segments we

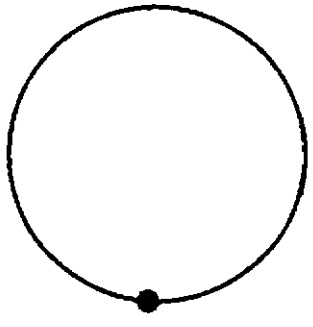

Figure A1. Closed loop, representing the lowest-order contribution to the renormalized fugacity, z_R. This diagram also represents the generating function for the number of unrestricted, closed walks.

must find the coefficient of z^{N_0} in $f(z_R)=f(z+uf(z))\approx f(z)+uf'(z)f(z)$. Using (A.1), (A.3) and (A.4) we find that the terms of order z^{N_0} sum up to

$$\left(\frac{z}{z_c}\right)^{N_0}\left(\frac{1}{N_0\delta}\left(\left(1+(N_0+1)\frac{u}{z_c}\right)+\frac{u}{z_c}\sum_{m=1}^{N_0-2}\frac{N_0-m}{m(N_0-m-1)}\right)\right)$$
$$\approx\left(\frac{z}{z_c}\right)^{N_0}\left(\frac{1}{N_0\delta}\left(\left(1+\frac{u}{z_c}\right)^{N_0+1}+\frac{u}{z_c}\ln N_0\right)\right). \tag{A.5}$$

If the inequality in (A.2) is satisfied, the last term in the brackets can be neglected, and the expression for the number of walks is dominated by contributions behaving qualitatively like the expression for the number of walks in the absence of self-avoidance, i.e. the right-hand side of (A.3). When N_0 is large, the factor in (A.5) depending on the ratio u/z_c can be absorbed into a multiplicative renormalization of z_c.

It remains to be established that the criterion embodied in the inequality (A.2) for the irrelevance of self-avoidance in the vicinity of the 'popping' transition has a validity transcending the perturbation-theoretic derivation of this appendix.

References

Aronovitz J and Nelson D R 1986 *J. Physique* **47** 1445
Camacho J and Fisher M E 1990 *Phys. Rev. Lett.* **65** 9
Canham P B 1970 *J. Theor. Biol.* **26** 61
Deuling H J and Helfrich W 1976 *J. Physique* **37** 1335
Diehl H W and Eisenregler E 1989 *J. Phys. A: Math. Gen.* **22** L87
Edwards S F 1973 *Molecular Fluids* ed R Balian and G Weil (London: Gordon and Breach)
Fixman M 1962 *J. Chem. Phys.* **36** 306
Flory P J 1971 *Principles of Polymer Physics* (Ithaca, NY: Cornell University Press)
Forsman W and Hughes R 1963 *J. Chem. Phys.* **38** 2118
Gaspari G, Rudnick J and Beldjenna A 1987 *J. Phys. A: Math. Gen.* **20** 3393
Gaspari G, Rudnick J and Fauver M 1993 *J. Phys. A: Math. Gen.* **26** 15
Helfrich W 1973 *Z. Naturforsch.* **28C** 693
Leibler S, Singh R P R and Fisher M E 1987 *Phys. Rev. Lett.* **59** 1989
Leibler S 1989 *Statistical Mechanics of Membranes and Surfaces* ed D R Nelson, T Piran and S Weinberg (Singapore: World Scientific)
Levinson E 1992 *Phys. Rev.* A **45** 3629
Maggs A C, Leibler S, Fisher M E and Camacho J 1991 *Phys. Rev.* A **72** 691
Ostrowsky N and Peyrand J 1982 *J. Chem. Phys.* **77** 2081
Rouse P E 1953 *J. Chem. Phys.* **21** 1272
Rudnick J and Gaspari G 1986 *J. Phys. A: Math. Gen.* **19** L191
—— 1991 *Science* **252** 422
Solĉ K 1971 *J. Chem. Phys.* **55** 335
Solĉ K and Gobush W 1974 *Macromolecules* **7** 814
Solĉ K and Stockmayer W H 1971 *J. Chem. Phys.* **54** 2756
Theodoru D and Suter U 1985 *Macromolecules* **18** 1206